Semi-Annual Status Report

Submitted to:	NASA Langley Research Center
Grant Title:	ROBUST STABILITY OF SECOND-ORDER SYSTEMS
Grant Number:	NAG-1-1397
Organization:	Georgia Institute of Technology Atlanta, GA 30332-0150
Principal Investigator:	Dr. C.-H. Chuang School of Aerospace Engineering Georgia Institute of Technology Atlanta, GA 30332-0150 (404) 894-3075
Period Covered:	Feb. 24, 1993 to Aug. 23, 1993
Date of Submission:	Aug. 19, 1993

TABLE OF CONTENTS

A PASSIVITY BASED CONTROLLER FOR SPACE MANIPULATORS

Abstract

A feedback linearization technique is used in conjunction with passivity concepts to design robust controllers for space robots. It is assumed that bounded modeling uncertainties exist in the inertia matrix and the vector representing the coriolis, centripetal, and friction forces. Under these assumptions, the controller guarantees asymptotic tracking of the joint variables. A Lagrangian approach is used to develop a dynamic model for space robots. Closed-loop simulation results are illustrated for a simple case of a single link planar space manipulator with freely floating base.

1. Introduction

The dynamics of the space manipulators differs from that of the ground based manipulators since their base, the spacecraft, is free to move. The movement of the manipulator produces reaction forces and torques on the base. Therefore the resulting motion of the spacecraft has to be accounted for in the dynamic model for the manipulator. However, Papadopoulos and Dubowsky [1] showed that a dynamic model for space robots developed by taking into account the motion of its base is similar in structure to dynamic models of fixed base manipulators. For instance, the inertia matrix in each case is symmetric and positive definite.

A few concepts have been proposed for joint trajectory control and inertial end tip motion control of space manipulators. Vafa and Dubowsky [2] developed an analytical tool for space manipulators, known as the virtual manipulator concept. The virtual manipulator is an idealized kinematic chain connecting its base, the virtual base, to any point on the real manipulator. This point can be chosen to be the manipulator's end effector, while the virtual base is located at the system center of mass, which is fixed in inertial space. As the real manipulator moves, the end of the virtual manipulator remains coincident with the selected point on the real manipulator. Additionally, it can be shown that the change in orientation in the virtual manipulator's joints is equal to the change in the orientation of the real manipulator's joints. While these features give the designer the ability to represent a free floating space manipulator by a simpler system whose base is fixed in inertial space, the associated transformation depends on knowing the system parameters exactly. Alexander and Cannon [3] showed that the end tip of the space robot can be controlled by solving the inverse dynamics that includes motion of the base. Their method assumes the mass of the spacecraft to be relatively large compared to that of the manipulator it carries, and also requires much computational effort to determine the control input. Note that, future systems are expected to have the manipulator and spacecraft masses of the same order. Umetani and Yoshida [4] proposed the generalized Jacobian matrix that

relates the end tip velocities to the joint velocities by taking into account the motion of the base. The control method presented in the above reference is based on the concept of Resolved Motion Rate Control and Resolved Acceleration Control. However, robustness of the control scheme to modeling uncertainties is not discussed. Masutani et. al. [5] proposed a sensory feedback control scheme based on an artificial potential defined in the sensor coordinate frame. This scheme is based on proportional feedback of errors in the end tip position and orientation as well as feedback of joint angular velocities.

In this report a robust control scheme based on feedback linearization and passivity concepts is proposed for space robots. A similar control scheme has been proposed earlier for fixed base robots by Abdallah and Jordan [6]. The extension to space robots is in the spirit of the [1], where it was proposed that due to the striking similarity in the structure of the equations of motion of fixed base and space robots; almost any control scheme used for fixed base robots can be applied to space robots. The control scheme uses inverse dynamics; however, it is robust in the face of bounded modeling uncertainties which might be due to imprecise modeling and/or intentional simplifications to the model based control law in order to reduce computational effort. The controller asymptotically tracks prescribed time varying joint angle trajectories whose acceleration is bounded in the L^2 space.

2. Dynamics of Space Manipulator System without Attitude Control of the Base

The development of the equations of motion for space robots presented here closely follows that given in [5]. A space manipulator system in the satellite orbit can be approximately considered to be floating in a non-gravitational environment. As shown in Figure 1, the manipulator and the base can be treated as a set of n+1 rigid bodies connected through n joints. The bodies are numbered from zero to n with the base being 0 and the end tip being n. Each joint is then numbered accordingly from one to n. The angular displacements of the joints can be represented by a joint vector,

$$q = [q_1 \; q_2 \cdots q_n]^T \tag{1}$$

The mass and inertia tensor of the i^{th} body are denoted by m_i and I_i, and the inertia tensor is expressed in the base frame coordinates.

2.1 Kinematics

A coordinate frame fixed to the orbit of the satellite can be considered to be an inertial frame, denoted by Σ_I. In addition to Σ_I, another coordinate frame Σ_B is defined that is attached to the base with its origin located at the base center of mass. The attitude of the base itself is given by roll, pitch, and yaw angles. In the sequel, all vectors are expressed in the base fixed coordinate axes.

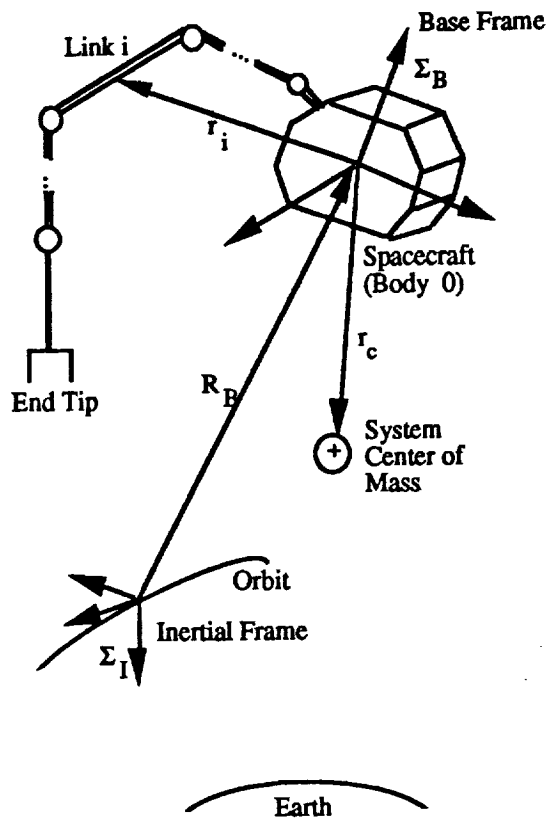

Figure 1. A Space Robot.

Let V_i be the linear velocity of the center of mass of the i^{th} link with respect to the inertial frame. Also, for the i^{th} link, let Ω_i be the angular velocities with respect to the inertial frame, and let ω_i be the angular velocity with respect to the base frame. Then V_i and Ω_i can be written as

$$V_i = V_B + v_i + \Omega_B \times r_i \tag{2}$$

$$\Omega_i = \Omega_B + \omega_i \tag{3}$$

where r_i is the position vector of the center of mass of the i^{th} body with respect to the base center of mass, and $v_i = \dot{r}_i$. V_B and Ω_B are the center of mass linear velocity and angular velocity respectively of the base with respect to the inertial frame. v_i and ω_i for each link can be represented by the following forms

$$v_i = J_{Li}(q)\dot{q} \tag{4}$$

$$\omega_i = J_{Ai}(q)\dot{q} \tag{5}$$

where $J_{Li}(q)$ and $J_{Ai}(q) \in R^{3xn}$ are the Jacobian matrices for the i^{th} link .

The position of the system center of mass with respect to the base frame depends on the joint angles. Given below are two measures related to the system center of mass

$$m_c = \sum_{i=0}^{n} m_i \tag{6}$$

$$r_c(q) = \sum_{i=0}^{n} m_i r_i(q)/m_c \tag{7}$$

2.2 Dynamics

The total kinetic energy of the space robot can be written as

$$T = \frac{1}{2}\dot{q}^T D(q)\dot{q}, \quad D \in R^{n\times n} \tag{8}$$

where D is the inertia matrix of the system and is given by

$$D = H_q - \begin{bmatrix} H_{vq}^T & H_{\Omega q}^T \end{bmatrix} \begin{bmatrix} H_v & H_{v\Omega} \\ H_{v\Omega}^T & H_\Omega \end{bmatrix}^{-1} \begin{bmatrix} H_{vq} \\ H_{\Omega q} \end{bmatrix} \tag{9}$$

It can be shown that $D = D^T > 0$. H_q is the inertia matrix corresponding to the fixed base manipulator

$$H_q = \sum_{i=1}^{n} \left[m_i J_{Li}^T J_{Li} + J_{Ai}^T I_i J_{Ai} \right], \quad H_q \in R^{n\times n} \tag{10}$$

The second term on the right hand side of Equation (9) arises due to the fact that the base of the space robot is free. Since the working environment is non-gravitational and no actuators generating external forces are employed, the linear and angular momenta of the whole system are conserved. Since the inertial frame is fixed to the orbit, the whole system can be assumed to be stationary with respect to the inertial frame at the initial state. Thus the above two momenta are always zero for the whole system. Note that it is implicitly implied that the satellite is a non-spinning body. Using the assumption of zero initial momenta the individual components comprising the second term on the right hand side of Equation (9) can be written as

$$H_v = m_c I_{3\times3} \ , \ H_v \in R^{3\times3} \tag{11}$$

$$H_\Omega = \sum_{i=0}^{n} I_i + \sum_{i=1}^{n} m_i [r_i\times]^T [r_i\times], \ H_\Omega \in R^{3\times3} \tag{12}$$

$$H_{v\Omega} = -m_c [r_c\times], \ H_{v\Omega} \in R^{3\times3} \tag{13}$$

$$H_{vq} = \sum_{i=1}^{n} m_i J_{Li}, \quad H_{vq} \in R^{3\times n} \tag{14}$$

$$H_{\Omega q} = \sum_{i=1}^{n} \{I_i J_{Ai} + m_i [r_i\times] J_{Li}\}, \quad H_{\Omega q} \in R^{3\times n} \tag{15}$$

where for any vector

$$f = \begin{pmatrix} f_1 \\ f_2 \\ f_3 \end{pmatrix} \tag{16}$$

$$[f\times] \equiv \begin{pmatrix} 0 & -f_3 & f_2 \\ f_3 & 0 & -f_1 \\ -f_2 & f_1 & 0 \end{pmatrix} \tag{17}$$

and I_{3x3} is the 3x3 identity matrix.

Since there is no potential energy in non-gravitational environment, the Lagrangian, Λ, is equal to the kinetic energy

$$\Lambda = T \tag{18}$$

So the system dynamics is given by

$$\frac{d}{dt}\left(\frac{\partial \Lambda}{\partial \dot{q}}\right) - \frac{\partial \Lambda}{\partial q} = \tau \tag{19}$$

where τ is an nx1 vector of input torques. Paralleling the development for fixed base robots given by Spong and Vidyasagar [7], the equations of motion for space robots can be written as,

$$D(q)\ddot{q} + h(q,\dot{q}) = \tau \quad . \tag{20}$$

where

$$h(q,\dot{q}) = C(q,\dot{q})\dot{q} \tag{21}$$

and the elements of the matrix C are given by

$$C_{kj} = \frac{1}{2}\sum_{i=1}^{n}\left\{\frac{\partial D_{kj}}{\partial q_i} + \frac{\partial D_{ki}}{\partial q_j} - \frac{\partial D_{ij}}{\partial q_k}\right\}\dot{q}_i \tag{22}$$

2.3 Base Motion

The conservation of linear and angular momenta yields expressions for the base translational and angular velocities

$$\begin{bmatrix} V_B \\ \Omega_B \end{bmatrix} = -\begin{bmatrix} H_v & H_{v\Omega} \\ H_{v\Omega}^T & H_\Omega \end{bmatrix}^{-1}\begin{bmatrix} H_{vq} \\ H_{\Omega q} \end{bmatrix}\dot{q} \tag{23}$$

Using the above expressions, the evolution of the base position and orientation with time can be determined as follows

$$\begin{bmatrix} \dot{x}_b \\ \dot{y}_b \\ \dot{z}_b \end{bmatrix} = \begin{bmatrix} c_\psi c_\theta & c_\psi s_\theta s_\phi - s_\psi c_\phi & c_\psi s_\theta c_\phi + s_\psi s_\phi \\ s_\psi c_\theta & s_\psi s_\theta s_\phi + c_\psi c_\phi & s_\psi s_\theta c_\phi - c_\psi s_\phi \\ -s_\theta & c_\theta s_\phi & c_\theta c_\phi \end{bmatrix} V_B \tag{24}$$

$$\begin{bmatrix} \dot{\phi} \\ \dot{\theta} \\ \dot{\psi} \end{bmatrix} = \begin{bmatrix} 1 & s_\phi \tan(\theta) & c_\phi \tan(\theta) \\ 0 & c_\phi & -s_\phi \\ 0 & s_\phi \sec(\theta) & c_\phi \sec(\theta) \end{bmatrix} \Omega_B \tag{25}$$

where

$$c_{(\cdot)} \equiv \cos(\cdot)\,,\; s_{(\cdot)} \equiv \sin(\cdot) \tag{26}$$

3. Control System Design

3.1 Feedback Linearization

Assuming that the dynamics of the space robot is described by Equation (20), where D and h are completely known, the feedback linearization or inverse dynamics technique [7] can be used to design controllers for tracking prescribed command trajectories for the joint angles. This can be accomplished by letting

$$\tau = Du + h \tag{27}$$

where u is the pseudo-control, i.e., it is the control input to the linearized system. With the control law given by Equation (27), the closed-loop system becomes

$$\begin{Bmatrix} \dot{q} \\ \ddot{q} \end{Bmatrix} = A \begin{Bmatrix} q \\ \dot{q} \end{Bmatrix} + Bu \tag{28}$$

where

$$A = \begin{bmatrix} 0 & I \\ 0 & 0 \end{bmatrix}, B = \begin{bmatrix} 0 \\ I \end{bmatrix} \tag{29}$$

A simple PD (Proportional-Derivative) type of control law is chosen for the feedback linearized system

$$u = \ddot{q}_d + K_2(\dot{q}_d - \dot{q}) + K_1(q_d - q) \tag{30}$$

where K_1 and K_2 are proportional and derivative gain matrices, respectively. These matrices are usually chosen to be diagonal in order to achieve decoupled response among the joint angles. Substituting for u from Equation (30) into Equation (28), one obtains

$$\dot{e} = A_c e \tag{31}$$

where $e = \{e_1^T \; e_2^T\}^T$, $e_1 = q_d - q$, $e_2 = \dot{q}_d - \dot{q}$, $A_c = A - BK$, and $K = [K_1 \;\; K_2]$. If $K_1 > 0$ and $K_2 > 0$, the error dynamics as given by Equation (31) is asymptotically stable. The freedom in selecting the gain matrices can be utilized to meet performance specifications for the closed-loop system.

The preceding discussion assumes availability of perfect knowledge about the system dynamics. However, in practice, D and h are usually imprecisely known due to modeling inaccuracies. Furthermore, D and h may be too

complex to be used for real-time control implementation. In the following sub-section, a control law that is robust for bounded uncertainties in D and h is given. The control law results in closed-loop asymptotic tracking.

3.2 Robust Feedback Linearization Using Passivity

The development in this section follows that given in [6] very closely. In the presence of modeling uncertainties, the control law is given as

$$\tau = D_c u + h_c \tag{32}$$

where D_c and h_c are computed versions of D and h respectively. Substituting for τ and u from Equations (32) and (30) into Equation (20) it can be shown that the closed-loop system dynamics is given by

$$\dot{e} = A_c e + Bv \tag{33}$$

where

$$v = \Delta u + \delta \tag{34}$$

and

$$\Delta = (I - D^{-1}D_c),\ \delta = D^{-1}(h - h_c) \tag{35}$$

The first step in the design proposed in [6] is to choose the gain matrix $K = [K_1\ \ K_2]$ and an output matrix F such that the linear system given by

$$\begin{aligned} \dot{e} &= A_c e + Bv \\ y &= Fe \end{aligned} \tag{36}$$

is SPR (Strictly Positive Real). This can be achieved as outlined in the following theorem. A definition of the concept of Strictly Positive Realness can be found in Slotine and Li [8].

Theorem 1 [6]. Let K_1 and K_2 be such that

$$\begin{aligned} K_1 &= \text{diag}[k_{1i}];\ k_{1i} > 0, i = 1,\ldots,n \\ K_2 &= \text{diag}[k_{2i}];\ k_{2i} > 0, i = 1,\ldots,n \\ (k_{2i})^2 &> k_{1i}, \qquad i = 1,\ldots,n \end{aligned} \tag{37}$$

then if F = K, the system described by Equation (36) is SPR.

The proof is omitted here, the interested reader is referred to [6]. Note that the conditions of the theorem given in Equations (37) are extremely easy to satisfy.

With the linear system (37) being SPR, the passivity theorem (Desoer and Vidyasagar, [9]) can be used to design asymptotically stable controllers as shown in the following theorem. The theorem is very similar to that given in [6], with the only difference being in the way in which the uncertainty bound on the h vector is characterized. The notation $\|x\|_T = \left(\int_0^T x^T x\, dt\right)^{1/2}$ is used in the sequel.

Theorem 2. Let the following two inequalities hold

$$D \le \frac{1}{r} I \quad (r > 0) \tag{38}$$

$$\|D^{-1}(h - h_c)\|_T \le c\|u\|_T + d \quad \forall T > 0 \quad (c \ge 0, \infty > d \ge 0) \tag{39}$$

Furthermore, let $\ddot{q}_d \in L^2$. Then if $D_c = aI$ where

$$a > \frac{c+1}{r} \tag{40}$$

the closed-loop system is asymptotically stable.

Proof. The closed-loop system as given by Equation (33) can be represented in block diagram form as shown in Figure 2. It is first shown that the nonlinear block in the feedback path is passive [9].

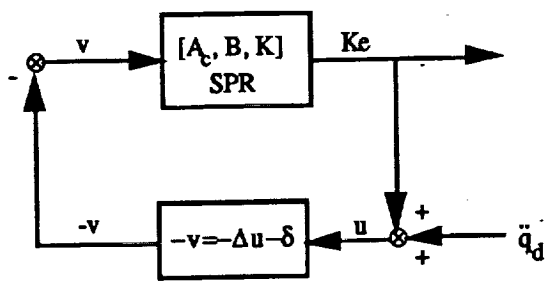

Figure 2. Robust Feedback Linearization Using Passivity Theorem.

Consider

$$
\begin{aligned}
I &= \int_0^T -u^T v dt \quad (T > 0) \\
&= \int_0^T -u^T (\Delta u + \delta) dt \\
&= \left(-\int_0^T u^T \Delta u dt \right) + \left(-\int_0^T u^T \delta dt \right)
\end{aligned} \tag{41}
$$

Let the first and second integrals on the right hand side be denoted by I_1 and I_2 respectively. Then

$$
I_1 = \int_0^T u^T (aD^{-1} - I) u \, dt \tag{42}
$$

Noting that

$$
D \le \frac{1}{r} I \quad \Rightarrow \quad aD^{-1} - I \ge (ar - 1) I \tag{43}
$$

one can obtain

$$
I_1 \ge (ar - 1) \|u\|_T^2 \tag{44}
$$

On the other hand,

$$
\begin{aligned}
-I_2 &= \int_0^T u^T D^{-1} (h - h_c) dt \\
&\le \|u\|_T \left\| D^{-1} (h - h_c) \right\|_T \quad \text{(Hölder's Inequality)} \\
&\le \|u\|_T [c \|u\|_T + d]
\end{aligned} \tag{45}
$$

Hence

$$
I \ge (ar - c - 1) \|u\|_T^2 - d \|u\|_T = f\left(\|u\|_T \right) \tag{46}
$$

It can be shown that if (ar - c - 1) > 0, then

$$
f\left(\|u\|_T \right) \ge -\frac{d^2}{4(ar - c - 1)} \quad \forall \ \|u\|_T \ge 0 \tag{47}
$$

Hence

$$\int_0^T -u^T v\,dt \geq -\frac{d^2}{4(ar-c-1)} \quad \forall T>0 \tag{48}$$

Thus a sufficient condition for the nonlinear block to be passive is that $a > (c + 1)/r$.

Additionally, the transfer function of the feedforward block $[A_C, B, K]$ is proper and has no poles on the imaginary axis. Hence it has finite gain (Doyle, Francis, and Tannenbaum, [10]). Since $\ddot{q}_d \in L^2$, then using the passivity theorem [9], one can conclude that the signals u, Ke, and v are bounded. Moreover, since the feedforward block is SPR, $Ke(t) = K_1e_1(t) + K_2e_2(t)$ goes to zero asymptotically. This in turn implies that $e_1(t)$ and $e_2(t)$ individually approach zero asymptotically [8].

The first condition of the theorem, given by Equation (38), is easy to satisfy since D is upper bounded. However, the second condition, given by Equation (39), might not be easy to verify in a straightforward manner in all applications.

4. Simulation Results

As an example, results are illustrated for a single link space robot shown in Figure 3. Equation (20) describes the dynamics of this one degree of freedom system. The system inertia, computed using Equation (9), turns out to be

$$D(q_1) = m'P_1^2 + I_1 - \frac{1}{d}[m'P_1(P_0c_1 + P_1) + I_1]^2 \tag{49}$$

where

$$d = m'(P_o^2 + P_1^2 + 2P_oP_1c_1) + I_o + I_1 \tag{50}$$

and $m' = m_0m_1 / (m_0 + m_1)$. Using Equations (21) and (22), h is determined to be

$$h(q_1, \dot{q}_1) = \frac{m'P_oP_1s_1}{d^2}[m'P_o(P_o + P_1c_1) + I_o]\cdot[m'P_1(P_oc_1 + P_1) + I_1]\dot{q}_1^2 \tag{51}$$

In Equations (49) through (51), $c_1 \equiv \cos(q_1), s_1 \equiv \sin(q_1)$.

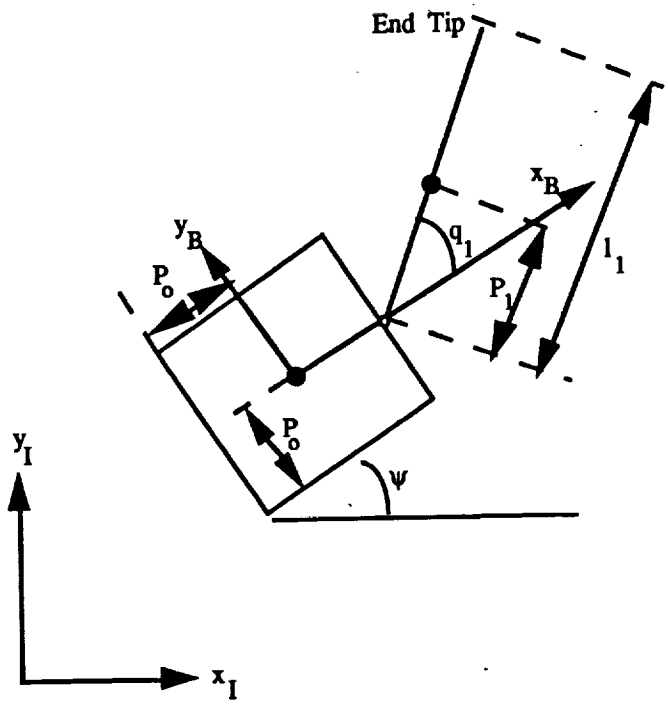

Figure 3. A Single Link Planar Space Robot.

It can be seen easily that as $m_0 \to \infty$, and $I_0 \to \infty$,

$$D \to m_1 P_1^2 + I_1, \; h \to 0 \tag{52}$$

which represents the case of a fixed base manipulator. Equation (24) is used to determine the evolution of the base position with time

$$\dot{x}_b = \frac{m'}{m_0}\left[P_1 s_{\psi 1} - \frac{1}{d}\left\{m' P_1 (P_o c_1 + P_1) + I_1\right\} \cdot \left(P_1 s_{\psi 1} + P_o s_\psi\right)\right]\dot{q}_1$$

$$\dot{y}_b = \frac{m'}{m_0}\left[-P_1 c_{\psi 1} + \frac{1}{d}\left\{m' P_1 (P_o c_1 + P_1) + I_1\right\} \cdot \left(P_1 c_{\psi 1} + P_o c_\psi\right)\right]\dot{q}_1 \tag{53}$$

where

$$s_{\psi 1} = \sin(\psi + q_1), \; c_{\psi 1} = \cos(\psi + q_1) \tag{54}$$

Finally, the base attitude dynamics is obtained using Equation (25)

$$\dot{\psi} = -\frac{1}{d}\left[m'P_1(P_o c_1 + P_1) + I_1\right]\dot{q}_1 \tag{55}$$

Next, a feedback controller is designed for the space robot using the results of Theorems 1 and 2. Closed-loop results are generated for a step command of 1 radian to the joint angle. Note that in general, for end tip motion control in the inertial space, the inverse kinematics problem needs to be solved to generate a command trajectory for the joint angle. Table 1 lists physical parameters of the example robot used in simulation. The base and link masses are of the same order of magnitude. The feedback gains are chosen to be $k_1 = 0.4$ and $k_2 = 1.0$. This choice of gains satisfies Equations (37) and in case of no modeling uncertainty, yields a closed-loop response without any overshoot. The fact that the system center of mass should remain stationary in inertial space is used to monitor the step-size of integration to achieve numerical accuracy. Simulation results are shown for the case in which there is no modeling uncertainty, and for two other cases that involve differing degrees of uncertainty. It is assumed that Equations (20) and (49) through (51) represent the true robot; the uncertainty is introduced in computing D and h. An upper bound for the system inertia, needed for condition (39) of Theorem 2, is given for this particular case by

$$\frac{1}{r} = m'P_1^2 + I_1 \tag{56}$$

a in Theorem 2 is assumed to be $1.1/r$ for both cases involving uncertainty. The choice of h_c however, is different for the two cases. In the first case, the following simplification to h is used for computing the closed-loop control

$$h_c = m'P_o P_1 s_1 \dot{q}_1 \tag{57}$$

The second case corresponds to an even greater simplification to h

$$h_c = m'P_o P_1 \dot{q}_1 \tag{58}$$

Figures 4 through 7 show closed-loop results for the nominal case and for the first case involving uncertainty. c = 0.01 was chosen to satisfy condition (41) of Theorem 2. d was chosen to be 2.5. Figure 4 shows that asymptotic tracking in the joint angle is achieved in the face of uncertainty. This is associated with a slight performance

Table 1. Physical Parameters of Example Robot.

Body	P (meter)	l (meter)	m (kg)	I (kg.m^2)
0 (Base)	3.0	-	5.0	30.0
1 (Link)	3.0	6.0	1.0	3.0

degradation in the joint angle response in the sense that it has an overshoot. Figure 5 shows that higher magnitudes of joint torque are required for the case involving uncertainty. Figures 4 and 6 show that the base moves in reaction to link motion; this is due to the conservation of linear and angular momentum as discussed previously. However, the joint angle still achieves the right commanded value. Figure 7 shows that the choice of c and d used in this case satisfies condition (40) of Theorem 2.

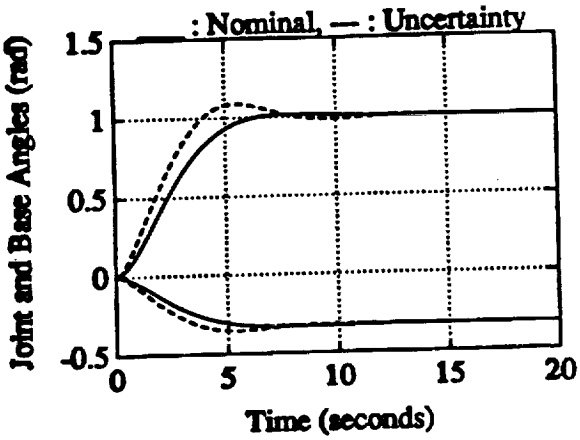

Figure 4. Joint and Base Angle Responses for the Nominal Case and the First Case Involving Uncertainty.

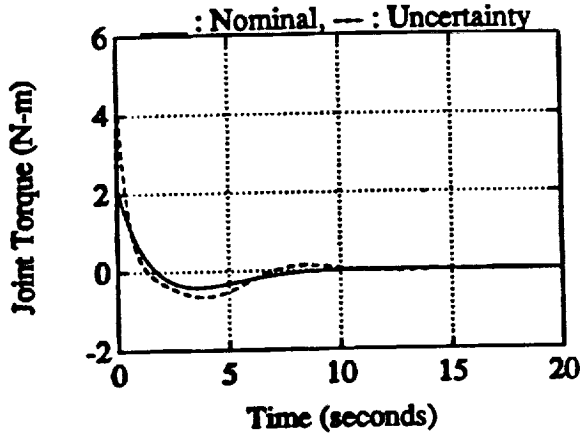

Figure 5. Joint Torque Input for the Nominal Case and the First Case Involving Uncertainty.

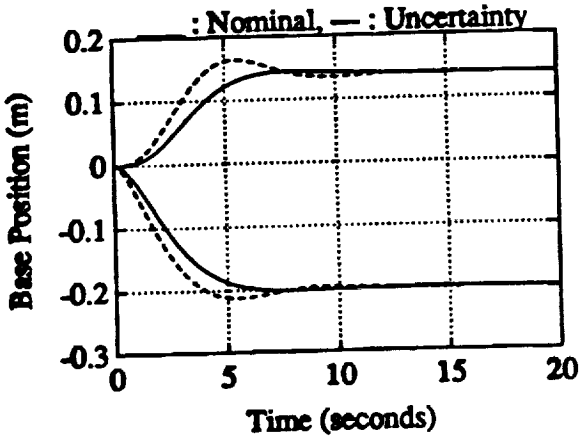

Figure 6. Motion of the Base Center of Mass for the Nominal Case and the First Case Involving Uncertainty.

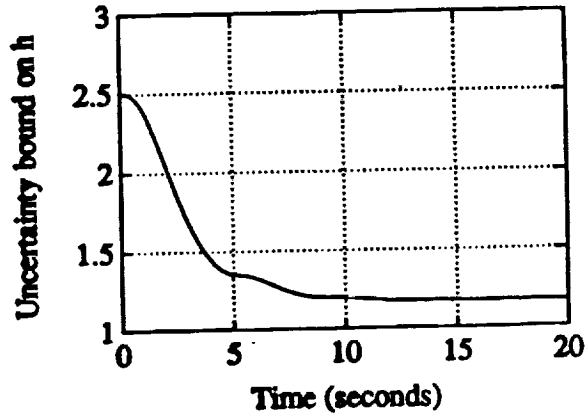

Figure 7. $c\|u\|_T + d - \|D^{-1}(h - h_c)\|_T$ for the Nominal Case and the First Case Involving Uncertainty.

Figures 8 through 11 show closed-loop results for the nominal case and the second case involving uncertainty. For the second case, c and d are chosen to be c = 0.01 and d = 5.0. Trends similar to the previous case are noticed here also. However, since the extent of uncertainty is greater, there is more deviation in the responses as compared to the previous case. This is observed in Figures 8 through 10. Figure 11 confirms that the choice of c and d satisfies the requirements of Theorem 2.

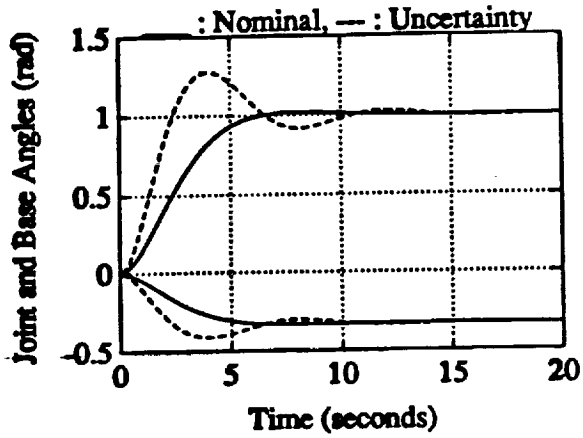

Figure 8. Joint and Base Angle Responses for the Nominal Case and the Second Case Involving Uncertainty.

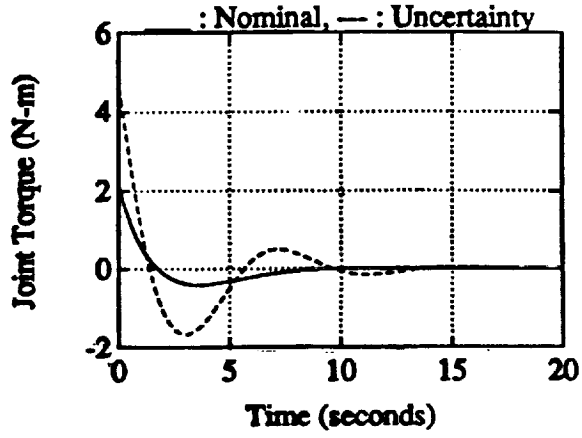

Figure 9. Joint Torque Input for the Nominal Case and the Second Case Involving Uncertainty.

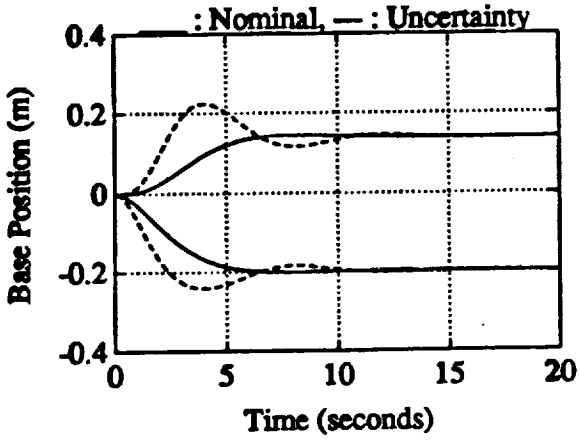

Figure 10. Motion of the Base Center of Mass for the Nominal Case and the Second Case Involving Uncertainty.

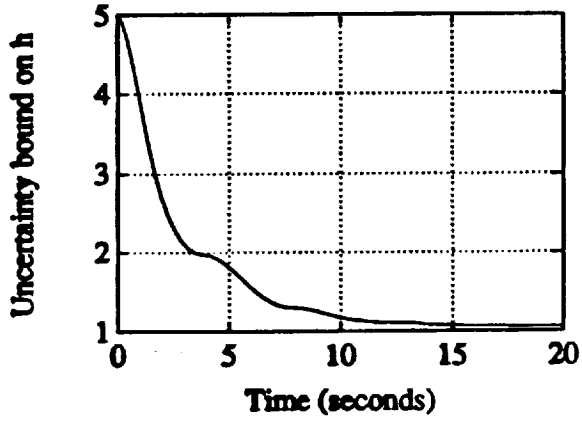

Figure 11. $c\|u\|_T + d - \|D^{-1}(h - \dot{h}_c)\|_T$ for the Nominal Case and the Second Case Involving Uncertainty.

5. Conclusions

A control method based on feedback linearization and passivity concepts that was proposed earlier for fixed base robots is modified and extended to the case of space robots. The control law results in asymptotic joint angle tracking in the face of bounded uncertainties. For the first time, closed-loop simulation results are presented using this control method. For the simple example illustrated in the report, the control method shows promising results.

References

[1]. E. Papadopoulos and S. Dubowsky, "On the Nature of Control Algorithms for Space Manipulators," Proceedings of the 1990 IEEE International Conference on Robotics and Automation, Cincinnati, Ohio, pp. 1102-1108.

[2]. Z. Vafa and S. Dubowsky, "The Kinematics and Dynamics of Space Manipulators: The Virtual Manipulator Approach," The International Journal of Robotics Research, Raleigh, 9(4), August 1990.

[3]. H. L. Alexander and R.H. Cannon, "Experiments on the Control of a Satellite Manipulator," Proceedings of the 1987 American Control Conference, Minneapolis, Minnesota.

[4]. K. Yoshida and Y. Umetani, "Control of Space Manipulators with Generalized Jacobian Matrix," Space Robotics: Dynamics and Control, edited by Y. Xu and T. Kanade, Kluwer Academic Publishers, 1993 pp. 165-204.

[5]. Y. Masutani, F. Miyazaki, and S. Arimoto, "Sensory Feedback Control For Space Manipulators," Proceedings of the 1989 IEEE International Conference on Robotics and Automation, Scottsdale, Arizona.

[6]. C. Abdallah and R. Jordan, "A Positive-Real Design for Robotic Manipulators," Proceedings of the 1990 American Control Conference, San Diego, California, pp. 991-992.

[7]. M. W. Spong and M. Vidyasagar, Robot Dynamics and Control, John Wiley, New York, 1989.

[8]. J-J. E. Slotine and W. Li, Applied Nonlinear Control, Prentice Hall, New Jersey, 1991, pp. 127, 399.

[9]. C. A. Desoer and M. Vidyasagar, Feedback Systems: Input-Output Properties, Academic Press, New York, 1975, pp. 173-186.

[10]. J. C. Doyle, B. A. Francis, and A. R. Tannenbaum, Feedback Control Theory, Macmillan, New York, 1992, pp. 16.